CONTENTS

Todo list

I Superconductivity

At the end of the 19th and the beginning of the 20th century, cooling technology made great progress. Liquifying gases, were able to reach temperatures as low as $4\,\mathrm{K}$ (the boiling point of Helium). Using that, SC was discovered in mercury in 1911 by Heike Onnes [1]. Superconductivity describes the phenomenon of the electrical resistance of a material suddenly dropping to zero below a critical temperature T_C. Discovery of Meissner effect, perfect expulsion of external magnetic fields in 1933 [2]. This started almost half a century of intensive theoretical research, which culminated in John Bardeen, Leon Cooper and J. Robert Schrieffer developing the microscopic theory now know as BCS theory [3]. 1986 and 1987: discovery of superconductivity with very high T_C found in cuprates [4, 5]. Cuprate superconductors are made up of layers of cooper oxide and charge reservoirs in between. The specific charge reservoir layers determine the properties of the SC and varying them lead to a rich zoo of materials with high T_C [6].

Most current technical applications of superconductors rely on the fact that superconducting wires can carry much higher currents that ordinary wires and thus produce much larger magnetic fields. The largest commercial application to date is in magnetic resonance imaging, a medical technique using strong magnetic fields and field gradients [7]. Technical applications in research are much wider, ranging from strong superconducting magnets in the LHC [8] and other particle accelerators over detectors of single photons in astrophysics [9] to extremely sensitive measurement devices for magnetic fields [10, 11].

Since the first discovery of SC in cuprates, there has been a lot of work to develop superconductors with higher transition temperatures. One interesting development in is in twisted multilayer systems, first realized as twisted bilayer Graphene [12]. In comparison to the complex crystal structure of e.g. the Cuprates, twisted multilayer systems have a very simple structure and can be tuned very easily: the angle of twist between the layers can be easily accessed experimentally. The defining feature of these systems are flat electronic bands

due to folding of the Brilluoin zone. Superconductivity in these systems is enhanced due to the fact that in the flat bands, interactions between the electrons are very strongly enhanced. Thus these systems are a very interesting playground to study strongly correlation effects in general and superconductivity in particular.

This chapter: introduction to the mean-field BCS theory in section I.3, GL-theory in section I.1 and

I.1 Ginzburg-Landau theory of superconductivity

Following [13, ch. 11].

I.1.1 Order parameter concept

Landau theory: phase transitions (e.g. iron becomes magnetic, water freezes, superfluidity/superconductivity) are associated with the development of an order parameter when the temperature drops below the transition temperature T_C.

$$|\psi| = \begin{cases} 0 \, , \, T > T_C \\ |\psi_0| > 0 \, , \, T < T_C \end{cases} \tag{I.1}$$

Landau theory does not need microscopic expression for order parameter, it provides corse-grained description of the properties of matter. The order parameter description is good at length scales above ξ_0, the coherence length (e.g. size of Cooper pairs for SC).

I.1.2 Ginzburg-Landau theory

Landau theory   Basic idea of Landau theory: write free energy as function $F[\psi]$ of the order parameter. Region of small ψ, expand free energy of many-body system as simple polynomial:

$$f_L = \frac{1}{V}F[\psi] = \frac{r}{2}\psi^2 + \frac{u}{4}\psi^4 \tag{I.2}$$

Provided r and u are greater that 0: minimum of $f_L[\psi])$ lies at $\psi = 0$. Landau theory assumes: at phase transition temperature r changes sign, so:

$$r = a(T - T_C) \tag{I.3}$$

Minimum of free energy occurs for:

$$\psi = \begin{cases} 0 \\ \pm\sqrt{\frac{a(T_C - T)}{u}} \end{cases} \tag{I.4}$$

Two minima for free energy function for $T < T_C$. With this, we can extract T_C from the knowledge of the dependence of $|\psi|^2$ on T via a linear fit. This is only valid for an area near T_C (where Landau theory holds), but can be used to get T_C from microscopic theories.

Going from a one to a n-component order parameters, OP acquires directions and magnitude. Particularly important example: complex or two component order parameter in superfluids and superconductors:

$$\psi = \psi_1 + i\psi_2 = |\psi|e^{i\phi} \tag{I.5}$$

The Landau free energy takes the form:

$$f[\psi] = r(\psi^*\psi) + \frac{u}{2}(\psi^*\psi)^2 \tag{I.6}$$

As before:

$$r = a(T - T_C) \tag{I.7}$$

Figure I.1 shows the Landau free energy as function of ψ.

Rotational symmetry, because free energy is independent of the global phase of the OP:

$$f[\psi] = f[e^{ia}\psi] \tag{I.8}$$

In this 'Mexican hat' potential: order parameter can be rotated continuously from one broken-symmetry state to another. If we want the phase to be rigid, we need to introduce an There is a topological argument for the fact that the phase is rigid. This leads to Ginzburg-Landau theory. Will see later: well-defined phase is associated with persistent currents or superflow.
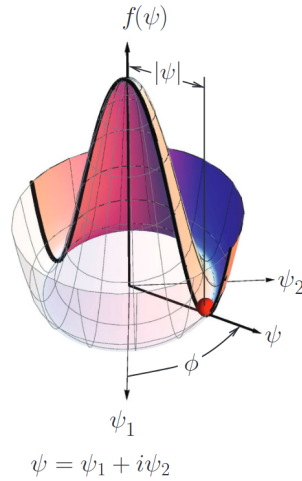
$f(\psi)$

$|\psi|$

ψ_2

ψ

ϕ

ψ_1

$\psi = \psi_1 + i\psi_2$

Figure I.1: *Mexican hat potential*

GINZBURG-LANDAU THEORY   Landau theory: energy cost of a uniform order parameter, more general theory needs to account for inhomogenous order parameters, in which the amplitude varies or direction of order parameter is twisted -> GL theory. First: one-component, 'Ising' order parameter. GL introduces additional energy $\delta f \propto |\Delta\psi|^2$, $f_{GL}[\psi, \Delta\psi] = \frac{s}{2}|\Delta\psi|^2 + f_L[\psi(s)]$, or in full:

$$f_{GL}[\psi, \Delta\psi, h] = \frac{s}{2}(\Delta\psi)^2 + \frac{r}{2}\psi^2 + \frac{u}{4}\psi^4 \tag{I.9}$$

GL theory is only valid near critical point, where OP is small enough to permit leading-order expansion. Length scale introduced by the gradient term: correlation length

$$d \tag{I.10}$$

length scale/correlation length

COMPLEX ORDER AND SUPERFLOW   Now: GL theory of complex or two-component order parameters, so superfluids and superconductors. Heart of discussion: emergence of a 'macroscopic wavefunction', where the microscopic field operators $\hat{\psi}(x)$ acquire an expectation value:

$$\langle \hat{\psi}(x) \rangle = \psi(x) = |\psi(x)|e^{i\theta(x)} \tag{I.11}$$

Reminder: Field operators are the real space representations of creation/annihilation operators. They can be thought of the super position of all ways of creating a particle at position x via the basis coefficients.

Magnitude determines density of particles in the superfluid:

$$|\psi(x)|^2 = n_s(x) \tag{I.12}$$

Density operator is

$$\hat{\rho} = \hat{\psi}(x)\hat{\psi}^\dagger(x) \tag{I.13}$$

so expectation value of that is the formula above.

Twist/gradient of phase determines superfluid velocity:

$$\mathbf{v}_s(x) = \frac{\hbar}{m}\Delta\phi(x) \tag{I.14}$$

We will derive this later in the chapter. Counterintuitive from quantum mechanics: GL suggested that $\Phi(x)$ is a macroscopic manifestation of a macroscopic number of particles condensed into precisely the same quantum state. Emergent phenomenon, collective properties of mater not a-priori self-evident from microscopic physics.

GL free energy density for superfluid (with one added term in comparison to Landau energy):

$$f_{GL}[\psi, \Delta\psi] = \frac{\hbar^2}{2m}|\Delta\psi|^2 + r|\psi|^2 + \frac{u}{2}|\psi|^4 \tag{I.15}$$

Interpreted as energy density of a condensate of bosons in which the field operator behaves as a complex order parameter. Gives interpretation of gradient term as kinetic energy:

energy density of bosonic field? -> for comparison!

$$s|\Delta\psi|^2 = \frac{\hbar^2}{2m}\langle\Delta\hat{\psi}^\dagger\Delta\hat{\psi}\rangle \implies s = \frac{\hbar^2}{2m} \tag{I.16}$$

As in Ising order: correlation length/GL-coherence length governs characteristic range of amplitude fluctuations of the order parameter:

$$\xi = \sqrt{\frac{s}{|r|}} = \sqrt{\frac{\hbar^2}{2m|r|}} = \xi_0(1 - \frac{T}{T_C})^{-\frac{1}{2}} \tag{I.17}$$

where $\xi_0 = \xi(T = 0) = \sqrt{\frac{\hbar^2}{2ma T_C}}$ is the coherence length. Beyond this length: only phase fluctuations survive. Freeze out fluctuations in amplitude (no x-dependence in amplitude) $\psi(x) = \sqrt{n_s}e^{i\phi(x)}$, then $\Delta\psi = i\Delta\phi\psi$ and $|\Delta\psi|^2 = n_s(\Delta\phi)^2$, dependency of kinetic energy on the phase twist is (bringing it into the form $\frac{m}{2}v^2$):

$$\frac{\hbar^2 n_s}{2m}(\Delta\phi)^2 = \frac{mn_s}{2}\left(\frac{\hbar}{m}\Delta\phi\right)^2 \tag{I.18}$$

So twist of phase results in increase in kinetic energy, associated with a superfluid velocity:

$$\mathbf{v}_s = \frac{\hbar}{m}\Delta\phi \tag{I.19}$$

For interpretation of superfluid states: coherent states. These are eigenstates of the field operator

$$\hat{\psi}(x)\,|\psi\rangle = \psi(x)\,|\psi\rangle \tag{I.20}$$

and don't have a definite particle number. Importantly, this small uncertainty in particle number enables a high degree of precision in phase (which is the property of a condensate).

Phase rigidity and superflow: in GL theory, energy is sensitive to a twist of the phase. Substitute $\psi = |\psi|e^{i\phi}$ into GL free energy, gradient term is:

$$\Delta\psi = (\Delta|\psi| + i\Delta\phi|\psi|)e^{i\phi} \tag{I.21}$$

So:

$$f_{GL} = \frac{\hbar}{2m}|\psi|^2(\Delta\phi)^2 + \left[\frac{\hbar}{2m}(\Delta|\psi|)^2 + r|\psi|^2 + \frac{u}{2}|\psi|^4\right] \tag{I.22}$$

The second term resembles GL functional for an Ising order parameter, describes energy cost of variations in the magnitude of the order parameter.

Here: particle-current operator, especially for coherent state, connection with phase twist

I.2 Superconducting length scales from the constraint of finite-momentum pairing

From [14].

In most materials: Cooper pairs do not carry finite center-of-mass momentum. In presence of e.g. external fields or magnetism: SC states with FMP might arise.

Theory/procedure in the paper: enforce FMP states via constraints on pair-center-of-mass momentum $\mathbf{q}$, access characteristic lenght scales ξ_0, λ_L through analysis of the momentum and temperature-dependent OP. Constrain for FF-type pairing:

$$\psi_{\mathbf{q}}(\mathbf{r}) = |\psi_{\mathbf{q}}|e^{i\mathbf{q}\mathbf{r}} \qquad (I.23)$$

> Finish up the discussion of Niklas paper

I.3 MEAN-FIELD THEORY OF SUPERCONDUCTIVITY

I.3.1 BCS THEORY

Following [13, ch. 14].

Theoretical description of SC: 1957 by John Bardeen, his postdoc Leon Cooper and the graduate in the group, J. Robert Schrieffer [3]. Description is based on the fact, that the Fermi sea is unstable towards development of bound pairs under arbitrarily small attraction [15]. These bound electrons show bosonic behaviour and

> Why supercurrent in BCS theory?

This model Hamiltonian

> BCS hamiltonian, pairing

The final element in this description was the origin of the attractive interaction between electrons, which Bardeen, Cooper and Schrieffer identified as a retarded electron-phonon interaction [3]. This so-called BCS-theory of superconductivity is very successful in explaining experimental results in many compounds, Surprisingly, it

> What is explained by phononic pairing

I.3.2 MEAN FIELD-THEORY ON THE ATTRACTIVE HUBBARD MODEL

Hubbard model is the simplest model for interactions

[16]

[17]

> Other pairing interactions can be taken, gives explanations for a lot of different SCs

MULTI-BAND BCS THEORY ON THE HUBBARD MODEL

> Some relevance of the repulsive Hubbard model

> Motivation for taking a negative U

> Phase diagram

> General multi-band mean field theory theory

How to solve mean field theory self-consistently

Self-consistent solution

How to include finite momentum

Finite momentum

II Quantum Metric

First formulated in [18]

Following Cheng - a pedagogical Introduction

Parameter dependent Hamiltonian $\{H(\lambda)\}$, smooth dependence on parameter $\lambda = (\lambda_1, \lambda_2, ...) \in \mathcal{M}$ (base manifold)

Hamiltonian acts on parametrized Hilbert space $\mathcal{H}(\lambda)$

Eigenenergies $E_n(\lambda)$, eigenstates $|\phi_n(\lambda)\rangle$

System state $|\psi(\lambda)\rangle$ is linear combination of $|\psi_n(\lambda)\rangle$ at every point in $\mathcal{M}$

Infinitesimal variation of the parameter $d\lambda$:

$$ds^2 = \|\psi(\lambda+d\lambda)-(\lambda)\|^2 = \langle\delta\psi|\delta\psi\rangle = \langle\partial_\mu\psi|\partial_\nu\psi\rangle\, d\lambda^\mu\, d\lambda^\nu = (\gamma_{\mu\nu}+i\sigma_{\mu\nu})\, d\lambda^\mu\, d\lambda^\nu$$
$$(\text{II.1})$$

Last part is splitting up into real and imaginary part

II.1 Quantum Metric and superfluid weight

[margin note: See what is specific to this paper, see that I can derive that myself]

[margin note: Dont get it here]

[margin note: Write up notes about quantum metric and superfluid weight]

9

III Dressed Graphene Model

III.1 Lattice Structure

Structure of honeycomb lattice following [19].

Monolayer graphene forms a honeycomb lattice, which is a hexagonal Bravais lattice with a two atom basis.
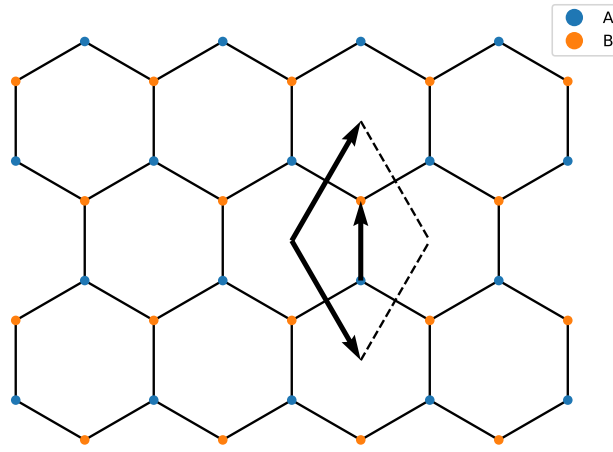

Figure III.1: *Graphene lattice structure*

Primitive lattice vectors of the hexagonal lattice:

$$\mathbf{a}_1 = \frac{a}{2} \begin{pmatrix} 1 \\ \sqrt{3} \end{pmatrix} \tag{III.1}$$

$$\mathbf{a}_2 = \frac{a}{2} \begin{pmatrix} 1 \\ -\sqrt{3} \end{pmatrix} \tag{III.2}$$

with lattice constant $a \approx 2.46$ Å (distance between unit cells). Have

$$a = \sqrt{3}a_0 \tag{III.3}$$

with the nearest-neighbour distance a_0.

Vectors to the nearest-neighbor B_i ($i = 1, 2, 3,$) atoms from atom A:

$$\delta_{AB,1} = \begin{pmatrix} 0 \\ \frac{a}{\sqrt{3}} \end{pmatrix}, \delta_{AB,2} = \begin{pmatrix} \frac{a}{2} \\ -\frac{a}{2\sqrt{3}} \end{pmatrix}, \delta_{AB,3} = \begin{pmatrix} -\frac{a}{2} \\ -\frac{a}{2\sqrt{3}} \end{pmatrix} \tag{III.4}$$

Vectors to the nearest-neighbor A_i ($i = 1, 2, 3,$) atoms from atom B:

$$\delta_{BA,1} = \begin{pmatrix} 0 \\ -\frac{a}{\sqrt{3}} \end{pmatrix}, \delta_{BA,2} = \begin{pmatrix} \frac{a}{2} \\ \frac{a}{2\sqrt{3}} \end{pmatrix}, \delta_{BA,3} = \begin{pmatrix} -\frac{a}{2} \\ \frac{a}{2\sqrt{3}} \end{pmatrix} \tag{III.5}$$

The vectors between the Graphene A atom and the six neighbours on the same sub lattice can be found by rotating $\mathbf{a}_1$ six times by $1/6 * 2\pi = \pi/3$:

$$\delta_{AA,1} = \mathbf{a}_1 = \frac{a}{2} \begin{pmatrix} 1 \\ \sqrt{3} \end{pmatrix} = a \begin{pmatrix} \frac{1}{2} \\ \frac{\sqrt{3}}{2} \end{pmatrix} = a \begin{pmatrix} \sin\left(\frac{\pi}{6}\right) \\ \cos\left(\frac{\pi}{6}\right) \end{pmatrix} \tag{III.6}$$

$$\delta_{AA,2} = a \begin{pmatrix} \sin\left(\frac{3\pi}{6}\right) \\ \cos\left(\frac{3\pi}{6}\right) \end{pmatrix} = a \begin{pmatrix} 1 \\ 0 \end{pmatrix} \tag{III.7}$$

$$\delta_{AA,3} = a \begin{pmatrix} \sin\left(\frac{5\pi}{6}\right) \\ \cos\left(\frac{5\pi}{6}\right) \end{pmatrix} = a \begin{pmatrix} \frac{1}{2} \\ -\frac{\sqrt{3}}{2} \end{pmatrix} \tag{III.8}$$

$$\delta_{AA,4} = a \begin{pmatrix} \sin\left(\frac{7\pi}{6}\right) \\ \cos\left(\frac{7\pi}{6}\right) \end{pmatrix} = a \begin{pmatrix} -\frac{1}{2} \\ -\frac{\sqrt{3}}{2} \end{pmatrix} \tag{III.9}$$

$$\delta_{AA,5} = a \begin{pmatrix} \sin\left(\frac{9\pi}{6}\right) \\ \cos\left(\frac{9\pi}{6}\right) \end{pmatrix} = a \begin{pmatrix} -1 \\ 0 \end{pmatrix} \tag{III.10}$$

$$\delta_{AA,6} = a \begin{pmatrix} \sin\left(\frac{11\pi}{6}\right) \\ \cos\left(\frac{11\pi}{6}\right) \end{pmatrix} = a \begin{pmatrix} -\frac{1}{2} \\ \frac{\sqrt{3}}{2} \end{pmatrix} \tag{III.11}$$

The primitive reciprocal lattice vectors $\mathbf{b}_1$, $\mathbf{b}_2$ fulfill

$$\mathbf{a}_1 \cdot \mathbf{b}_1 = \mathbf{a}_2 \cdot \mathbf{b}_2 = 2\pi \tag{III.12}$$

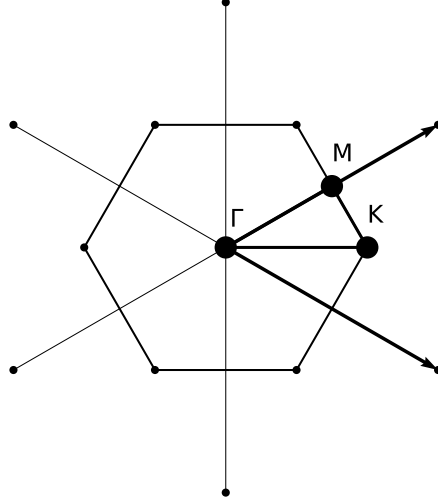$$\mathbf{a}_1 \cdot \mathbf{b}_2 = \mathbf{a}_2 \cdot \mathbf{b}_1 = 0 , \tag{III.13}$$

Figure III.2: *Graphene Brillouin Zone*

so we have:

$$\mathbf{b}_1 = \frac{2\pi}{a} \begin{pmatrix} 1 \\ \frac{1}{\sqrt{3}} \end{pmatrix} \tag{III.14}$$

$$\mathbf{b}_2 = \frac{2\pi}{a} \begin{pmatrix} 1 \\ -\frac{1}{\sqrt{3}} \end{pmatrix} \tag{III.15}$$

Points of high symmetry in the Brillouin zone are:

$$\Gamma = \begin{pmatrix} 0 \\ 0 \end{pmatrix} \tag{III.16}$$

$$M = \frac{\pi}{a} \begin{pmatrix} 1 \\ \frac{1}{\sqrt{3}} \end{pmatrix} \tag{III.17}$$

$$K = \frac{4\pi}{3a} \begin{pmatrix} 1 \\ 0 \end{pmatrix} \tag{III.18}$$

III.2 EG-X MODEL
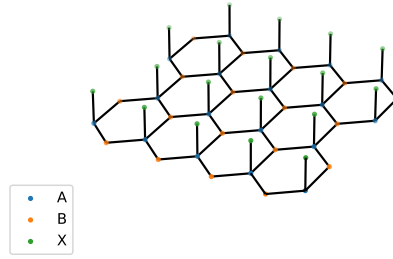
Graphene lattice and a site X.

Figure III.3: *EG-X model*

Without interaction:

$$H_0 = -t_X \sum_{\langle ij \rangle, \sigma} d_{i,\sigma}^\dagger d_{j,\sigma} - t_{Gr} \sum_{\langle ij \rangle, \sigma} c_{i,\sigma}^{(A),\dagger} c_{j,\sigma}^{(B)} + V \sum_{i,\sigma\sigma'} d_{i,\sigma}^\dagger c_{i,\sigma'}^{(A)} + \text{h.c.} \qquad \text{(III.19)}$$

with:

- d operators on the X atom
- $c^{(\epsilon)}$ operators on the graphene site ($\epsilon = A, B$)
- t_X NN hopping for X
- t_{Gr} NN hopping of Gr
- V hybridization between X and Graphene B sites

We can also introduce an onsite Hubbard interaction:

$$H_{\text{int}} = U_X \sum_i d_{i,\uparrow}^\dagger d_{i,\downarrow}^\dagger d_{i,\downarrow} d_{i,\uparrow} + U_{Gr} \sum_{i, \epsilon=A,B} c_{i,\uparrow}^{(\epsilon)\dagger} c_{i,\downarrow}^{(\epsilon)\dagger} c_{i,\downarrow}^\epsilon c_{i,\uparrow}^\epsilon \qquad \text{(III.20)}$$

> Write the Hamiltonian with orbital indeces

Define sublattice index

$$\alpha = 1, 2, 3 \tag{III.21}$$

with $1 \cong \text{Gr}_1, 2 \cong \text{Gr}_2, 3 \cong \text{X}$. Then we can write the non-interacting term as

$$H_0 = - \sum_{\langle i,j \rangle, \alpha, \beta, \sigma} [\mathbf{t}]_{i\alpha, j\beta} \, c_{i\alpha}^{\dagger} c_{j\beta} \tag{III.22}$$

with the matrix

$$\mathbf{t} = \begin{pmatrix} 0 & t_{\text{Gr}} & 0 \\ t_{\text{Gr}} & 0 & -V\delta_{ij} \\ 0 & -V\delta_{ij} & t_{\text{X}} \end{pmatrix} \tag{III.23}$$

Add chemical potential:

$$-\mu \sum_{i\alpha\sigma} n_{i\alpha\sigma} \tag{III.24}$$

Also write the interaction part with α (with changed signs compared to Niklas, to keep in line with papers about the attractive Hubbard model):

$$H_{int} = - \sum_{i\alpha} U_\alpha c_{i\alpha\uparrow}^{\dagger} c_{i\alpha\downarrow}^{\dagger} c_{i\alpha\downarrow} c_{i\alpha\uparrow} \tag{III.25}$$

III.2.1 REVIEW: HUBBARD MODEL ON THE HONEYCOMB LATTICE

> Write review for Hubbard model on the honeycomb lattice

III.2.2 BAND STRUCTURE OF THE NON-INTERACTING EG-X MODEL

To treat eq. III.19, we first write out the sums over nearest neighbours $\langle i,j \rangle$ explicitly, writing $\delta_{\text{X}}, \delta_\epsilon$ ($\epsilon = A, B$) for the connections to the nearest neighbours of the X atoms and Graphene A, B sites. Doing the calculation for the example of the X atoms:

$$- t_{\text{X}} \sum_{\langle ij \rangle, \sigma\sigma'} (d_{i,\sigma}^{\dagger} d_{j,\sigma'} + d_{j,\sigma}^{\dagger} d_{i,\sigma'}) \tag{III.26}$$

$$= -\frac{t_{\text{X}}}{2} \sum_{i,\sigma,\sigma'} \sum_{\delta_{\text{X}}} d_{i,\sigma}^{\dagger} d_{i+\delta_{\text{X}},\sigma'} - \frac{t_{\text{X}}}{2} \sum_{j,\sigma,\sigma'} \sum_{\delta_{\text{X}}} d_{j,\sigma}^{\dagger} d_{j+\delta_{\text{X}},\sigma'} \tag{III.27}$$

$$= -t_{\text{X}} \sum_{i,\sigma,\sigma'} \sum_{\delta_{\text{X}}} d_{i,\sigma}^{\dagger} d_{i+\delta_{\text{X}},\sigma'} \tag{III.28}$$

(The factor $1/2$ is to account for double counting when going to the sum over all lattice sites i)

Now we can input the discrete Fourier transform (for both graphene and X operators) into eq. III.28

$$c_i = \frac{1}{\sqrt{N}} \sum_{\mathbf{k}} e^{i\mathbf{k}\mathbf{r}_i} c_{\mathbf{k}} \tag{III.29}$$

$$c_i^\dagger = \frac{1}{\sqrt{N}} \sum_{\mathbf{k}} e^{-i\mathbf{k}\mathbf{r}_i} c_{\mathbf{k}}^\dagger \tag{III.30}$$

with the completeness relation:

$$\sum_i e^{i\mathbf{k}\mathbf{r}_i} e^{-i\mathbf{k}'\mathbf{r}_i} = N\delta_{\mathbf{k},\mathbf{k}'} . \tag{III.31}$$

We get:

$$-t_X \frac{1}{N} \sum_{i,\sigma,\sigma'} \sum_{\delta_X} d_{i,\sigma}^\dagger d_{i+\delta_X,\sigma'} = -t_X \frac{1}{N} \sum_{i,\sigma,\sigma'} \sum_{\delta_X} \sum_{\mathbf{k},\mathbf{k}'} e^{-i\mathbf{k}\mathbf{r}_i} d_{\mathbf{k},\sigma}^\dagger e^{i\mathbf{k}'\mathbf{r}_i} e^{i\mathbf{k}'\delta_X} d_{\mathbf{k}',\sigma'} \tag{III.32}$$

$$= -t_X \frac{1}{N} \sum_{\mathbf{k},\mathbf{k}',\sigma,\sigma'} \sum_{\delta_X} d_{\mathbf{k},\sigma}^\dagger e^{i\mathbf{k}'\delta_X} d_{\mathbf{k}',\sigma'} \sum_i e^{-i\mathbf{k}\mathbf{r}_i} e^{i\mathbf{k}'\mathbf{r}_i} \tag{III.33}$$

$$= -t_X \frac{1}{N} \sum_{\mathbf{k},\mathbf{k}',\sigma,\sigma'} \sum_{\delta_X} d_{\mathbf{k},\sigma}^\dagger e^{i\mathbf{k}'\delta_X} d_{\mathbf{k}',\sigma'} N\delta_{\mathbf{k},\mathbf{k}'} \tag{III.34}$$

$$= -t_X \sum_{\mathbf{k},\sigma,\sigma'} d_{\mathbf{k},\sigma}^\dagger d_{\mathbf{k},\sigma'} \sum_{\delta_X} e^{i\mathbf{k}\delta_X} \tag{III.35}$$

The nearest neighbours for X atoms are the vectors $\delta_{AA,i}$ from section III.1. With that, we can calculate:

$$f_X(\mathbf{k}) = -t_X \sum_{\delta_X} e^{i\mathbf{k}\delta_X} \tag{III.36}$$

$$= -t_X \left(e^{ia(\frac{k_x}{2} + \frac{\sqrt{3}k_y}{2})} + e^{iak_x} + e^{ia(\frac{k_x}{2} - \frac{\sqrt{3}k_y}{2})} \right. \tag{III.37}$$

$$\left. + e^{ia(-\frac{k_x}{2} - \frac{\sqrt{3}k_y}{2})} + e^{-iak_x} + e^{ia(-\frac{k_x}{2} + \frac{\sqrt{3}k_y}{2})} \right) \tag{III.38}$$

$$= -t_X \left(2\cos(ak_x) + 2e^{ia\frac{\sqrt{3}k_y}{2}}\cos(\frac{a}{2}k_x) + 2e^{-ia\frac{\sqrt{3}k_y}{2}}\cos(\frac{a}{2}k_x) \right) \tag{III.39}$$

$$= -2t_X \left(\cos(ak_x) + 2\cos(\frac{a}{2}k_x)\cos(\sqrt{3}\frac{a}{2}k_y) \right) \tag{III.40}$$

We can do the same for the hopping between Graphene sites, for example :

$$-t_{Gr} \sum_{\langle ij \rangle, \sigma\sigma'} c_{i,\sigma}^{(A),\dagger} c_{j,\sigma'}^{(B)} = -t_{Gr} \sum_{i,\sigma\sigma'} \sum_{\delta_{AB}} c_{i,\sigma}^{(A),\dagger} c_{i+\delta_{AB},\sigma'}^{(B)} \tag{III.41}$$

$$= -t_{Gr} \sum_{\mathbf{k},\sigma,\sigma'} c_{\mathbf{k},\sigma}^{(A)\dagger} c_{\mathbf{k},\sigma'}^{(B)} \sum_{\delta_{AB}} e^{i\mathbf{k}\delta_{AB}} \tag{III.42}$$

We note

$$\sum_{\delta_{AB}} e^{i\mathbf{k}\delta_{AB}} = \left(\sum_{\delta_{BA}} e^{i\mathbf{k}\delta_{BA}} \right)^* = \sum_{\delta_{BA}} e^{-i\mathbf{k}\delta_{BA}} \tag{III.43}$$

and calculate

$$f_{Gr} = -t_{Gr} \sum_{\delta_{AB}} e^{i\mathbf{k}\delta_{AB}} \tag{III.44}$$

$$= -t_{Gr} \left(e^{i\frac{a}{\sqrt{3}}k_y} + e^{i\frac{a}{2\sqrt{3}}(\sqrt{3}k_x - k_y)} + e^{i\frac{a}{2\sqrt{3}}(-\sqrt{3}k_x - k_y)} \right) \tag{III.45}$$

$$= -t_{Gr} \left(e^{i\frac{a}{\sqrt{3}}k_y} + e^{-i\frac{a}{2\sqrt{3}}k_y} \left(e^{i\frac{a}{2}k_x} + e^{-i\frac{a}{2}k_x} \right) \right) \tag{III.46}$$

$$= -t_{Gr} \left(e^{i\frac{a}{\sqrt{3}}k_y} + 2e^{-i\frac{a}{2\sqrt{3}}k_y}\cos(\frac{a}{2}k_x) \right) \tag{III.47}$$
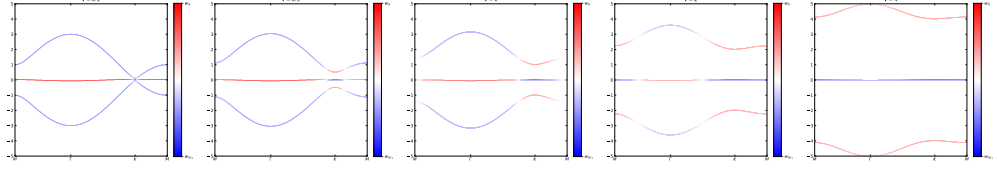
Figure III.4: *Bands of the non-interacting EG-X model. All the bands are spin-degenerate.*

All together, we get:

$$H_0 = \sum_{\mathbf{k},\sigma} \begin{pmatrix} c_{k,\sigma}^{A,\dagger} & c_{k,\sigma}^{B,\dagger} & d_{k,\sigma}^{\dagger} \end{pmatrix} \begin{pmatrix} 0 & f_{Gr} & V \\ f_{Gr}^* & 0 & 0 \\ V & 0 & f_X \end{pmatrix} \begin{pmatrix} c_{k,\sigma}^{A} \\ c_{k,\sigma}^{B} \\ d_{k,\sigma} \end{pmatrix} \tag{III.48}$$

The band structure for the non-interacting EG-X model is easily obtained by diagonalising the matrix in eq. III.48. This was done in fig. III.4.

Values used for calculation:

- $a_0 = 1$
- $t_{Gr} = 1$
- $t_X = 0.01$

V is the control parameter. (According to Niklas), a range from $V = 0.1$ to $V = 2$ can be mapped onto materials in experiment.

III.3 Multiband BCS?

Fourier transformation:

$$H_{int} = -\frac{1}{N^2} \sum_{\alpha,\mathbf{k}_{1,2,3,4}} U_\alpha e^{i(\mathbf{k}_1 + \mathbf{k}_4 - \mathbf{k}_1 - \mathbf{k}_3) r_{i\alpha}} c_{\mathbf{k}_1\alpha\uparrow}^\dagger c_{\mathbf{k}_3\alpha\downarrow}^\dagger c_{\mathbf{k}_2\alpha\downarrow} c_{\mathbf{k}_4\alpha\uparrow} \tag{III.49}$$

Impose zero-momentum pairing: $\mathbf{k}_1 + \mathbf{k}_3 = 0$ and $\mathbf{k}_2 + \mathbf{k}_4 = 0$:

$$H_{int} = -\sum_{\alpha,\mathbf{k},\mathbf{k}'} U_\alpha c_{\mathbf{k}\alpha\uparrow}^\dagger c_{-\mathbf{k}\alpha\downarrow}^\dagger c_{-\mathbf{k}'\alpha\downarrow} c_{\mathbf{k}'\alpha\uparrow} \tag{III.50}$$

Mean-field approximation:

$$H_{int} \approx \sum_{\alpha,\mathbf{k}} (\Delta_\alpha c^\dagger_{\mathbf{k}\alpha\uparrow} c^\dagger_{-\mathbf{k}\alpha\downarrow} + \Delta^*_\alpha c_{-\mathbf{k}\alpha\downarrow} c_{\mathbf{k}\alpha\uparrow}) \tag{III.51}$$

with

$$\Delta_\alpha = -U_\alpha \sum_{\mathbf{k'}} \langle c_{-\mathbf{k'}\alpha\downarrow} c_{\mathbf{k'}\alpha\uparrow} \rangle \tag{III.52}$$

$$\Delta^*_\alpha = -U_\alpha \sum_{\mathbf{k'}} \langle c^\dagger_{\mathbf{k'}\alpha\uparrow} c^\dagger_{-\mathbf{k'}\alpha\downarrow} \rangle \tag{III.53}$$

This gives the BCS mean field Hamiltonian:

$$H_{BCS} = \sum_{\mathbf{k}\alpha\beta\sigma} [H_{0,\sigma}(\mathbf{k})]_{\alpha\beta} c^\dagger_{\mathbf{k}\alpha\sigma} c_{\mathbf{k}\beta\sigma} - \mu \sum_{\mathbf{k}\alpha\sigma} n_{\mathbf{k}\alpha\sigma} + \sum_{\alpha,\mathbf{k}} (\Delta_\alpha c^\dagger_{\mathbf{k}\alpha\uparrow} c^\dagger_{-\mathbf{k}\alpha\downarrow} + \Delta^*_\alpha c_{-\mathbf{k}\alpha\downarrow} c_{\mathbf{k}\alpha\uparrow})$$
$$\tag{III.54}$$

with Nambu spinor

$$\Psi_{\mathbf{k}} = \begin{pmatrix} c_{1,\mathbf{k}\uparrow} \\ c_{2,\mathbf{k}\uparrow} \\ c_{3,\mathbf{k}\uparrow} \\ c^\dagger_{1,-\mathbf{k}\downarrow} \\ c^\dagger_{2,-\mathbf{k}\downarrow} \\ c^\dagger_{3,-\mathbf{k}\downarrow} \end{pmatrix} \tag{III.55}$$

we have:

$$H_{MF} = \sum_{\mathbf{k}} \Psi^\dagger_{\mathbf{k}} \mathcal{H}(\mathbf{k}) \Psi_{\mathbf{k}} \tag{III.56}$$

with

$$\mathcal{H}(\mathbf{k}) = \begin{pmatrix} H_{0,\uparrow}(\mathbf{k}) - \mu & \Delta \\ \Delta^\dagger & -H^*_{0,\downarrow}(-\mathbf{k}) + \mu \end{pmatrix} \tag{III.57}$$

with $H_{0,\sigma}$ being the F.T. of the kinetic term and $\Delta = diag(\Delta_1, \Delta_2, \Delta_3)$.

IV RESULTS

IV.1 GAPS

IV.2 SUPERFLUID WEIGHT

IV.3 BREAKDOWN OF SC WITH FINITE MOMENTUM

IV.4 COHERENCE LENGTH ETC.

Bibliography

[1] H. K. Onnes. "Further Experiments with Liquid Helium. G. On the Electrical Resistance of Pure Metals, Etc. VI. On the Sudden Change in the Rate at Which the Resistance of Mercury Disappears." In: *Through Measurement to Knowledge: The Selected Papers of Heike Kamerlingh Onnes 1853–1926*. Ed. by K. Gavroglu and Y. Goudaroulis. Dordrecht: Springer Netherlands, 1991, pp. 267–272. ISBN: 978-94-009-2079-8. DOI: `10.1007/978-94-009-2079-8_17` (cit. on p. 1).

[2] W. Meissner and R. Ochsenfeld. "Ein neuer Effekt bei Eintritt der Supraleitfähigkeit". In: *Naturwissenschaften* 21.44 (Nov. 1, 1933), pp. 787–788. ISSN: 1432-1904. DOI: `10.1007/BF01504252` (cit. on p. 1).

[3] J. Bardeen, L. N. Cooper, and J. R. Schrieffer. "Theory of Superconductivity". In: *Physical Review* 108.5 (Dec. 1, 1957), pp. 1175–1204. DOI: `10.1103/PhysRev.108.1175` (cit. on pp. 1, 7).

[4] J. G. Bednorz and K. A. Müller. "Possible High Tc Superconductivity in the Ba−La−Cu−O System". In: *Zeitschrift für Physik B Condensed Matter* 64.2 (June 1, 1986), pp. 189–193. ISSN: 1431-584X. DOI: `10.1007/BF01303701` (cit. on p. 1).

[5] S.-i. Uchida et al. "High Tc Superconductivity of La-Ba-Cu Oxides". In: *Japanese Journal of Applied Physics* 26 (1A Jan. 1, 1987), p. L1. ISSN: 1347-4065. DOI: `10.1143/JJAP.26.L1` (cit. on p. 1).

[6] D. Rybicki et al. "Perspective on the Phase Diagram of Cuprate High-Temperature Superconductors". In: *Nature Communications* 7.1 (May 6, 2016), p. 11413. ISSN: 2041-1723. DOI: `10.1038/ncomms11413` (cit. on p. 1).

[7] P. A. Rinck. *Magnetic Resonance in Medicine - A Critical Introduction*. ISBN: 978-628-01-2260-1. URL: `http://www.magnetic-resonance.org/` (cit. on p. 1).

[8] A. Tollestrup and E. Todesco. "The Development of Superconducting Magnets for Use in Particle Accelerators: From the Tevatron to the LHC". In: *Reviews of Accelerator Science and Technology* 1.01 (2008), pp. 185–210 (cit. on p. 1).

[9] K. Irwin and G. Hilton. "Transition-Edge Sensors". In: *Cryogenic Particle Detection*. Ed. by C. Enss. Berlin, Heidelberg: Springer, 2005, pp. 63–150. ISBN: 978-3-540-31478-3. DOI: 10.1007/10933596_3 (cit. on p. 1).

[10] D. Koelle et al. "High-Transition-Temperature Superconducting Quantum Interference Devices". In: *Reviews of Modern Physics* 71.3 (Apr. 1, 1999), pp. 631–686. DOI: 10.1103/RevModPhys.71.631 (cit. on p. 1).

[11] M. I. Faley et al. "High-Tc SQUID Biomagnetometers". In: *Superconductor Science and Technology* 30.8 (July 2017), p. 083001. ISSN: 0953-2048. DOI: 10.1088/1361-6668/aa73ad (cit. on p. 1).

[12] Y. Cao et al. "Unconventional Superconductivity in Magic-Angle Graphene Superlattices". In: *Nature* 556.7699 (Apr. 2018), pp. 43–50. ISSN: 1476-4687. DOI: 10.1038/nature26160 (cit. on p. 1).

[13] P. Coleman. *Introduction to Many-Body Physics*. Cambridge University Press, Nov. 2015. ISBN: 978-0-521-86488-6. DOI: 10.1017/CBO9781139020916 (cit. on pp. 2, 7).

[14] N. Witt et al. *Bypassing the Lattice BCS-BEC Crossover in Strongly Correlated Superconductors: Resilient Coherence from Multiorbital Physics*. July 11, 2024. DOI: 10.48550/arXiv.2310.09063. Pre-published (cit. on p. 6).

[15] L. N. Cooper. "Bound Electron Pairs in a Degenerate Fermi Gas". In: *Physical Review* 104.4 (Nov. 15, 1956), pp. 1189–1190. DOI: 10.1103/PhysRev.104.1189 (cit. on p. 7).

[16] M. Qin et al. "The Hubbard Model: A Computational Perspective". In: *Annual Review of Condensed Matter Physics* 13 (Volume 13, 2022 Mar. 10, 2022), pp. 275–302. ISSN: 1947-5454, 1947-5462. DOI: 10.1146/annurev-conmatphys-090921-033948 (cit. on p. 7).

[17] R. Micnas, J. Ranninger, and S. Robaszkiewicz. "Superconductivity in Narrow-Band Systems with Local Nonretarded Attractive Interactions". In: *Reviews of Modern Physics* 62.1 (Jan. 1, 1990), pp. 113–171. DOI: 10.1103/RevModPhys.62.113 (cit. on p. 7).

[18]   J. P. Provost and G. Vallee. "Riemannian Structure on Manifolds of Quantum States". In: *Communications in Mathematical Physics* 76.3 (Sept. 1, 1980), pp. 289–301. ISSN: 1432-0916. DOI: 10.1007/BF02193559 (cit. on p. 9).

[19]   G. Yang et al. "Structure of Graphene and Its Disorders: A Review". In: *Science and Technology of Advanced Materials* 19.1 (Aug. 29, 2018), pp. 613–648. ISSN: 1468-6996. DOI: 10.1080/14686996.2018.1494493 (cit. on p. 11).

LIST OF SYMBOLS